Modern glacimarine processes and potential future behaviour of Kronebreen and Kongsvegen polythermal tidewater glaciers, Kongsfjorden, Svalbard

Luke D. Trusel, R. D. Powell, R. M. Cumpston and J. Brigham-Grette

Email alerting service	click here to receive free email alerts when new articles cite this article
Permission request	click here to seek permission to re-use all or part of this article
Subscribe	click here to subscribe to Geological Society, London, Special Publications or the Lyell Collection

Notes

Modern glacimarine processes and potential future behaviour of Kronebreen and Kongsvegen polythermal tidewater glaciers, Kongsfjorden, Svalbard

LUKE D. TRUSEL[1,2]*, R. D. POWELL[1], R. M. CUMPSTON[1] & J. BRIGHAM-GRETTE[3]

[1]*Analytical Center for Climate and Environmental Change, Department of Geology and Environmental Geosciences, Northern Illinois University, 310 Davis Hall, Normal Rd., DeKalb, Illinois 60115, USA*

[2]*Present address: Graduate School of Geography, Clark University, 950 Main St., Worcester, Massachusetts 01610, USA*

[3]*Department of Geosciences, University of Massachusetts – Amherst, 611 N. Pleasant St., Morrill Science Center, Amherst, Massachusetts 01003, USA*

*Corresponding author (e-mail: ltrusel@clarku.edu)

Abstract: Glacimarine dynamics and associated sedimentary processes are closely tied to glacial regime and reflect dominant climatic conditions. Quantitative measurements for subpolar glaciers, such as sediment yield, are limited especially near glacial termini where most sediment accumulates. Here we characterize the modern glacimarine environment, quantify sediment flux and yield, document landform genesis and hypothesize potential future behaviour of Kronebreen and Kongsvegen glaciers in inner Kongsfjorden, Svalbard. A minimum of 6.74×10^3 g m^{-2} d^{-1} (at least 300 mm a^{-1}) of glacimarine sediment is building a grounding-line fan via submarine stream discharge from Kronebreen. Average daily sediment flux to the ice-contact basin is recorded to be 2.6×10^3 g m^{-2} d^{-1} or an average annual flux of 1.56×10^5 g m^{-2} a^{-1}. We measure an average annual ice-contact sediment yield of 1.20×10^4 tonnes km^{-2} a^{-1} associated with the rapid genesis of grounding-line landforms. With forecasted warming we expect meltwater volumes and sediment flux to increase. Grounding-line deposits may aggrade above water, tending to stabilize the terminus at least initially if the sediment is sufficient to counteract total terminus ablation. This would hold until either the glaciers next surge or climatic warming ablates the glaciers through surface melting.

The glaciers of western Spitsbergen, Svalbard are highly susceptible to climate fluctuations because of their intermediate position relative to the warm West Spitsbergen Current that transports Atlantic Water from the south and the colder Polar Water that flows from the north (Hald *et al.* 2004). Changes in freshwater flux from western Svalbard glaciers have many implications including influences on fjord sea ice, local biotas, fjord and river hydrology and, in extreme climate warming scenarios, a disturbance in deepwater production on the Svalbard shelf (Hagen *et al.* 2003). Sediment flux to marine grounding lines also has significant influences on glacial stability and potential future retreat or advance rates (Alley 1991; Powell 1991; Powell & Alley 1997; Fischer & Powell 1998; Alley *et al.* 2007). Because of amplified climatic warming at northern high latitudes (e.g. IPCC 2007), the glaciers of Spitsbergen, Svalbard are prime subjects for understanding not only glacial dynamics but also the effects of contemporary climate change.

Modern baseline measurements are fundamental and must be established to quantify the potential effects of climatic variability. Glacimarine processes such as sediment flux and yield, terminus fluctuations, calving rates, freshwater flux and mass-balance are useful for comparison among differing glacial and climatic regimes as well as for overall characterization of the state of the glacimarine system. Additionally, understanding the relationship of complex modern processes to those found in the glacimarine sediment record can enhance interpretation of past glacimarine processes and changes in biological productivity (Powell 1984).

The primary objective of this study is to characterize the modern ice-contact and ice-proximal

glacimarine environment of the Kronebreen-Kongs-vegen glacier complex (Fig. 1). We employ sediment flux records as well as fjord hydrographic and bathymetric profiling. This glacimarine system has been previously studied (e.g. Elverhøi *et al.* 1980, 1983; Svendsen *et al.* 2002) although extremely ice-proximal (within 1 km) measurements of sediment flux and water column properties are very limited. This understudied proximal zone is consequently the most dynamic, owing to the interplay of fresh meltwater discharge mixing with saline fjord water, rapid sediment flux and deposition, sediment slides and slumps, active calving and debris dumping, among other processes. Further, the confluent glacier complex has recently undergone pronounced changes including the emergence of Kongsvegen from tidewater. Post-surge quiescent phase conditions (cf. Meier & Post 1969) combined with significant meltwater and sediment fluxes have contributed to these conditions. Bathymetry near the termini reveals landforms that serve as records of ice-contact sediment flux. These measurements are the first of their kind in Kongsfjorden and represent the full potential of these subpolar glaciers in landscape denudation. We evaluate the modern system in relation to historical measurements and ultimately assess the ability of these glaciers to potentially influence their own future behaviour.
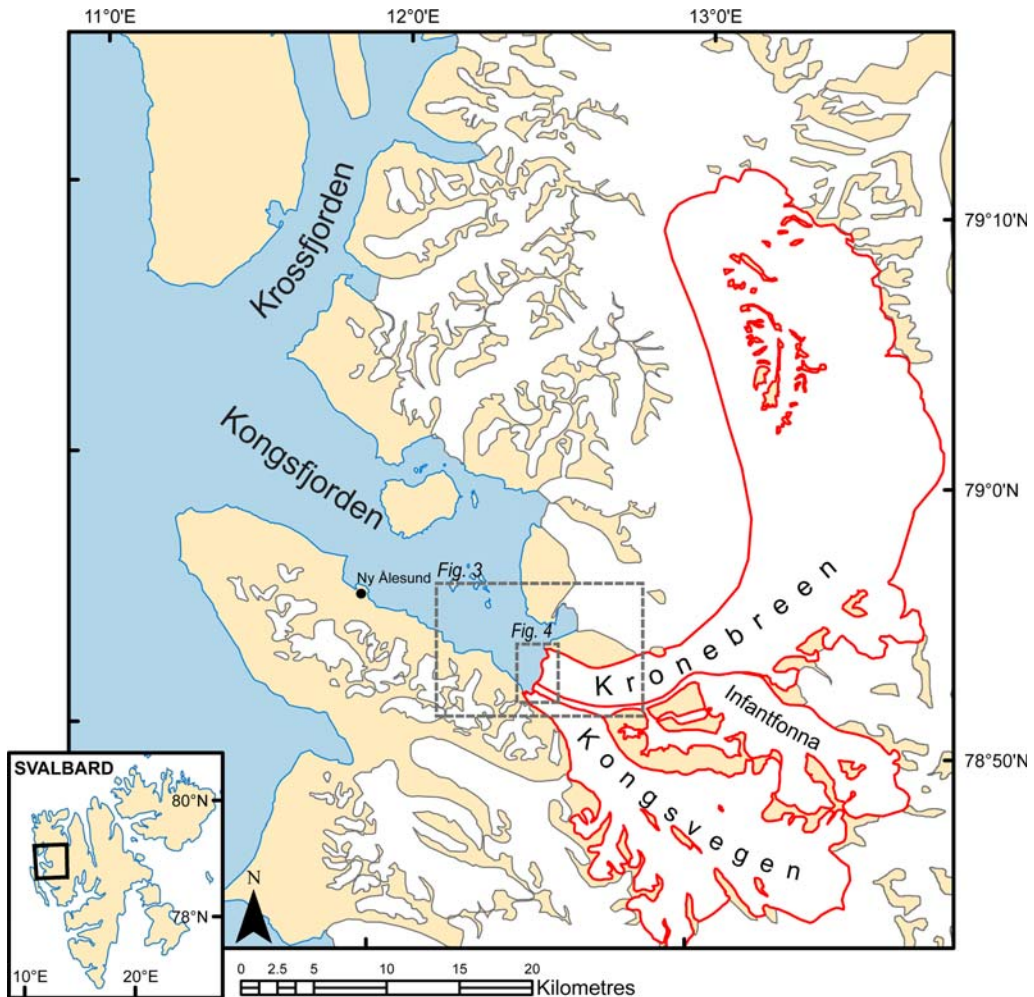

Fig. 1. Regional setting of Kongsfjorden and the glaciers of this study, Kronebreen and Kongsvegen as well as Infantfonna. Location of the large map is shown with respect to the islands of Svalbard in the inset map. Locations of additional figures indicated.

Study area

Physical setting

Kongsfjorden is a 22 km long and 4–12 km wide glacially eroded fjord in western Spitsbergen, Svalbard (Fig. 1). Fjord bathymetry is complex and variable, ranging from <60 m at its head to 400 m in several areas, separating the fjord into multiple distinct basins. Marine processes in Kongsfjorden are both spatially and temporally dynamic, characterized by a high degree of seasonality as is typical of arctic fjords (e.g. Syvitski 1989). Lacking a well-defined sill at its mouth (Howe *et al.* 2003), the fjord is highly interconnected with neighbouring water masses on the West Spitsbergen Shelf, including Atlantic Water (Svendsen *et al.* 2002), with influx particularly pronounced during midsummer (Cottier *et al.* 2005). Weather in the region is commonly unstable since Svalbard lies on the border-zone of cold Polar Basin circulation and warm maritime air masses from the south (Ingólfsson 2004). These conditions, combined with a seasonally abundant glacial meltwater flux, dictate both the physical (Svendsen *et al.* 2002; Gerland *et al.* 2004; MacLachlan *et al.* 2007) and biological (Hop *et al.* 2002) oceanography and make the Kongsfjorden area particularly susceptible to climate change (Lamb 1977).

Numerous subpolar, polythermal and surge-type tidewater glaciers calve into the fjord (e.g. Hagen *et al.* 1993) including the glaciers of this study, Kronebreen (445 km^2) and Kongsvegen (165 km^2) at the southeastern fjord head (Fig. 1). These glaciers join 5 km from their termini, forming a confluent glacier complex with Infantfonna (85 km^2) but with Kronebreen as the dominant tidewater cliff (Fig. 1). A recent widening of Kronebreen and the very slow, post-surge quiescent velocity of Kongsvegen (2.6 m a^{-1}) (Melvold & Hagen 1998) combined with its significant meltwater and sediment fluxes contributed to Kongsvegen emerging from tidewater between 1990 and 2005. Unlike Kongsvegen, Kronebreen has a high velocity of about 2 m d^{-1} (Hagen *et al.* 2003) or about 750 m a^{-1} (Melvold & Hagen 1998), providing evidence for sliding and melting at its bed to produce significant meltwater and sediment fluxes to the fjord (Svendsen *et al.* 2002). Bedrock strata underlying the complex include Devonian sandstone, conglomerate and localized marble, Carboniferous-Permian red sandstone, shale, coal and Proterozoic phyllite, carbonates and schists (Hjelle 1993). The length of the melt season for the Kronebreen-Kongsvegen complex is not directly known; however, the melt season for nearby terrestrial glaciers is documented at 60 days (Hodson *et al.* 1998).

Methodology

Field methods

All samples and data were collected from the inner basin of Kongsfjorden between July 18 and 31, 2005. Sample locations were sited using a hand-held GPS unit. Samples were collected from a 6 m aluminium skiff and 5 m inflatable boat.

Several devices were used to profile the marine water column in order to define its structure and potential paths of sediment transportation. Salinity and temperature were recorded and water density calculated by using a Sea-Bird SBE 19 CTD Profiler. The relative amount of suspended particulate matter within the water column was determined using a SeaTech transmissometer and an optical backscatter (OBS) device. A remotely triggered water sampler (2 L van Dorn bottle) was used to collect water samples from various fjord depths to quantify the suspended particulate matter (SPM) concentrations. Although the OBS and water samples measure total SPM, including both inorganic (siliciclastic) and organic (biologic) components, for simplicity we refer to total SPM as the 'suspended sediment' load because during summers the organic component is relatively very small (Svendsen *et al.* 2002).

Sediment traps were used as the primary measure of sediment flux and consequent rates of sedimentation from the subglacial stream discharges. Each trap was 250 mm × 48 mm and modelled after Cowan (1988), a trap design determined sufficient for quantitative sediment flux studies in Alaskan fjords. Each mooring was anchored to the bottom of the fjord and held relatively vertical using a rigid submersible float at about 10 m below low tide level to avoid iceberg interference. Each mooring had traps set at three depths: one near the surface (*c*. 15 m), a second in the middle of the water column (*c*. 25 m) and the third near the bottom (*c*. 50 m). At each depth an array of four individual cylindrical traps was set to assess error in trap measurements at each level in the water column. The bottom trap was located *c*. 5 m above the fjord floor, presumably high enough to avoid turbidity current activity, but low enough to accurately measure sediment being deposited on the fjord floor at each location.

Fjord bathymetry was determined using a Knudsen 320BP echosounder and sub-bottom profiler deployed along transects run across the fjord and following bearings approximately perpendicular to the ice cliff and the across-fjord lines. Points along transects were recorded using GPS-located coordinates.

Laboratory methods

Initial laboratory analyses were performed at the Arctic Marine Laboratory in Ny Ålesund, and were completed at the home institutions in the US.

Individual samples from sediment traps at each mooring were dried and the volume of collected sediment calculated. The dry sediment from these traps was weighed and used to calculate sedimentation rates per unit time. A Coulter LS-200 laser particle size analyser was used for particle size measurements.

Annual sedimentation rates were linearly extrapolated from trap measurements using the 60 day melt season of Hodson *et al.* (1998), derived from nearby terrestrial glaciers. This time span mediates a potentially pronounced midsummer meltwater flux (e.g. Svendsen *et al.* 2002) and the likelihood of longer melt seasons associated with the much thicker and more dynamic glaciers of this study. Sixty days are also significantly fewer than the average annual positive days between 2001 and 2008 (average 126 days per annum, most of which occur in summer) (Norwegian Meteorological Institute data from Ny Ålesund climate database website: http://eklima.met.no). Further evidence of a prolonged melt season comes from direct observations of meltwater effluent at the Kronebreen terminus during colder annual periods in autumn, winter and early spring, although this flux is thought to be rather infrequent and of low volume (Sund pers. comm. 2008). Therefore, although the Kronebreen-Kongsvegen ablation season is likely longer, for the purposes of conservative estimation a period of 60 days is used to calculate annual sediment flux.

Total volume of water in water samples was measured and the sediment within each sample was vacuum filtered using 63 μm Millipore filters. The resulting dry sediment was weighed and used to calculate suspended sediment concentrations in kg m^{-3}. These concentrations were also used to calibrate and convert OBS values into continuous kg m^{-3} measurements throughout the water column (Fig. 2). Two separate OBS calibration curves were generated based on different backscatter characteristics for sand particles as opposed to clay and silt. An upwelling-proximal calibration was therefore used in the vicinity of the Kronebreen point source with an r^2 of 0.9841; a Kongsvegen deltaic runoff calibration with an r^2 of 0.9844 was used for locations not in direct influence of the glacial upwelling (Fig. 2).

Recorded bathymetric points were interpolated using the Kriging method to create a continuous bathymetric map near the glacial termini. Recent terminus fluctuations were characterized using several datasets including satellite imagery and mapped terminus positions of other studies.

Results

Glacial retreat

The combined Kronebreen-Kongsvegen terminus has fluctuated over time and is most recently characterized by post-surge quiescent phase retreat. Retreat has been variable along the margin (Fig. 3), making the calculation of a retreat rate in kilometres per annum impractical. Available data, however, indicate overall terminus retreat rate has generally decreased following the recent maximum extension during the surge of 1948. The terminus has become almost stable since 1990, including a slight advance between 1999 and 2001.

This retreat has exposed a new sediment basin in the innermost fjord. Combined with recent quasi-stability, this has allowed for the generation of large submarine and subaerial morphological features that act as records of recent glacial sedimentary activity in the proximal basin.

Sedimentary landforms and denudation rates

A previously-undocumented ice-marginal, Gilbert-type delta has emerged in front of Kongsvegen, separating the glacier from tidewater (Figs 1, 3 & 4). The delta likely originated as a grounding-line fan at the former Kongsvegen tidewater terminus and, over time, built upon the southern fjord wall to eventually aggrade above sea level (e.g. Powell 1990). Photographs indicate the initial subaerial exposure of these deposits occurred before July 1996 (cf. Woodward *et al.* 2003, Fig. 1). From bathymetric soundings and satellite imagery we are able to accurately record the delta dimensions. The plain is measured at 0.33 km^2 and the delta-front slope extents 500 m into the fjord at a slope of 8°, terminating 70 m below sea level. Assuming the fjord wall on which the delta formed is at the same angle as the delta slope and a parallelogram delta-foreset configuration, we are able to geometrically estimate the volume. Using an average delta plain width of 350 m and the above dimensions, the cross-sectional area is calculated at 2.45×10^4 m^2. By multiplying by the average delta plain length of 800 m, total deltaic volume is estimated to be 1.96×10^7 m^3. Initial formation likely began immediately after Kongsvegen retreated over the western edge of the modern delta. Based on terminus positions mapped in Lefauconnier *et al.* (1994), initial uncovering of this area occurred in late summer 1983. Assuming growth over 22 years (1983–2005), its building rate is calculated to be 8.91×10^5 m^3 a^{-1}. Given that the total Kongsvegen drainage basin area is 210 km^2 with an average bedrock density of 2500 kg m^{-3} (primarily sedimentary rocks), this estimate provides a sediment yield of 1.06×10^4 tonnes km^{-2} a^{-1} (Table 1). This yield is equivalent to 4.24 mm a^{-1} bedrock erosion if 2500 tonnes km^{-2} is equal to 1 mm bedrock denudation (Table 1), following a similar methodology to Elverhøi *et al.* (1998).
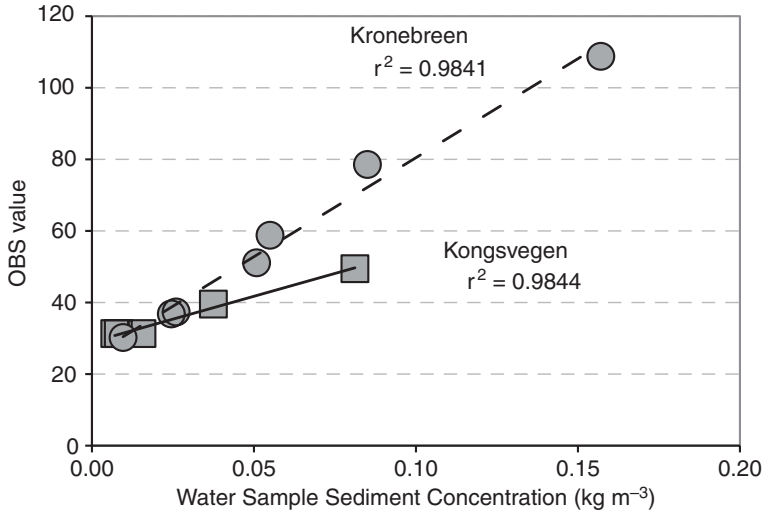
Fig. 2. Optical backscatter v. suspended-sediment concentrations and linear best-fit lines for Kronebreen (dashed line) and Kongsvegen (solid line). By relating measured sediment concentrations to OBS readings at specific depths and locations, we are able to infer sediment concentration from OBS.

Satellite, aerial and time-lapse imagery (Sund 2007) document the dynamic switching of submarine stream discharges at the Kronebreen-Kongsvegen margin. Available imagery from 1987, 1990, 1999 and 2000 reveal turbid upwelling adjacent to a recorded bathymetric high (B in Fig. 4). This submarine landform is interpreted as a grounding-line fan formed by those subglacial discharges (GLF in Fig. 4). In July 2005 the dominant meltwater upwelling was located about 500 m north along the terminus relative to its historical position (A in Fig. 4). High meltwater overflow velocities and frequent calving near the 2005 discharge prevented continuous acquisition of bathymetric data in this region. However, the inferred grounding-line fan appears to extend into the modern calving embayment, creating a continuous deposit with a minimum volume of 6.6×10^6 m^3. Assuming this

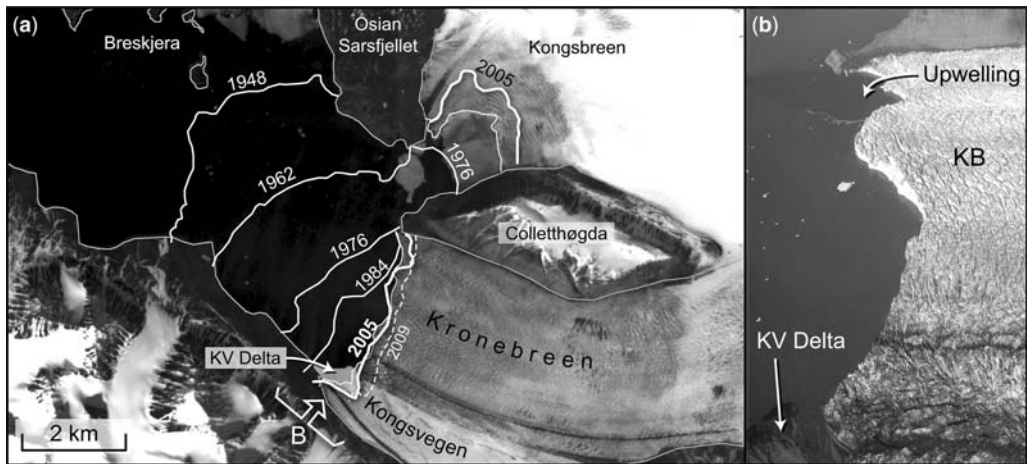**Fig. 3.** (**a**) Retreat of the glacial complex after its recent maximum extent during the surge of 1948. Mapping of terminus positions indicates that overall retreat rate has recently considerably slowed. (**b**) Oblique aerial photo taken in July 2005 showing the Kongsvegen delta in the foreground and the prominent submarine meltwater upwelling from Kronebreen in the distance. Arrow in (a) indicates the perspective view shown in (b). Figure extent shown in Figure 1.
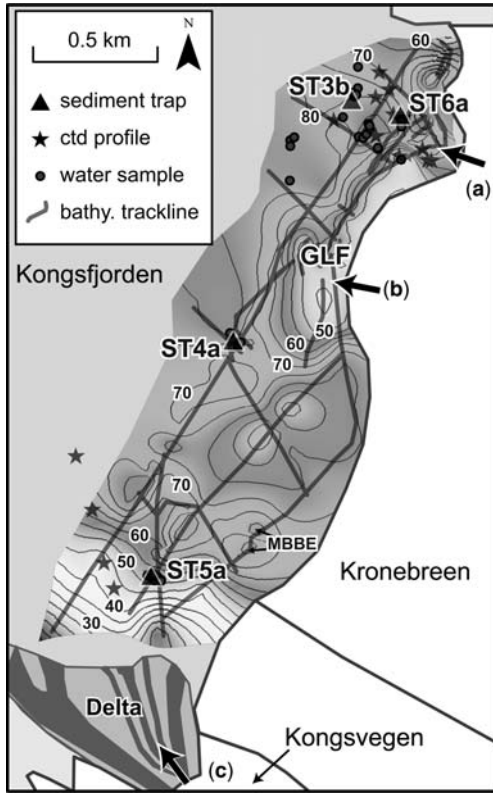
Fig. 4. Bathymetric and sample location map. Water depths are in metres with a 5 m contour interval. Bold arrows indicate modern and historical discharge point sources: (**a**) modern Kronebreen submarine stream discharge and upwelling; (**b**) historical discharge and upwelling location observed in available imagery from 1987, 1990, 1999 and 2000; and (**c**) modern Kongsvegen discharge source (GLF, grounding-line fan; MBBE, morainal bank bulls eyes).

deposit began accumulating *c.* 1984 when the terminus retreated to this location, a growth rate is calculated to be $3.3 \times 10^5 \, m^3 \, a^{-1}$. This rate equates to a sediment yield of 1.40×10^3 tonnes $km^{-2} \, a^{-1}$, equivalent to $0.56 \, mm \, a^{-1}$ of bedrock denudation (Table 1).

A semi-continuous bathymetric high at $60-70 \, m$ depth trends nearly north–south, parallel to the glacier termini, extending from the delta slope to the grounding-line fan. This feature may represent glaciotectonically thrusted sediments during winter, when calving is minimized and glacial flow results in net terminus advance (e.g. Elverhøi *et al.* 1980). Conversely, the ridge may indicate former subglacial discharge depocentres. Directly east of this high is a deeper basin extending to the ice face. Morainal bank 'bulls eyes' are especially obvious, associated with supraglacial dumping and englacial

meltout of the medial moraine formed where Kronebreen and Kongsvegen join (MBBE in Fig. 4).

Inner Kongsfjorden water column

The primary sediment source and driver of water column stratification is a meltwater upwelling from Kronebreen. As meltwater discharges from the base of the glacier, it entrains high concentrations of sediment and rapidly forms a turbulent jet (cf. Powell 1991). Because of relative density contrasts, the jet rises vertically and forms a buoyant and brackish surface overflow plume (SO water mass in Fig. 5). At the surface the brackish plume spreads laterally, confined mostly above 12 m depth as defined in hydrographic profiles (Fig. 5a). Water samples confirm that suspended sediment settles out of suspension through the entire water column in the glacier marginal zone. Suspended sediment concentrations peak between $0-4 \, m$ depth and, on average, decrease approximately logarithmically towards the fjord floor. The highest measured suspended sediment concentration in the overflow was $0.157 \, kg \, m^{-3}$; however, calibrated OBS measurements were as high as $0.266 \, kg \, m^{-3}$. The greatest variability in suspended concentrations occurs in the turbid overflow, with the highest dispersion occurring at the surface (Table 2; Fig. 5a).

The SO is on average colder, less saline and more sediment rich than ambient fjord water. Near the surface the SO is generally $0.5-1.0 \, °C$ and has salinities as low as 22‰ with a mean salinity of 30.96‰ in the upper 4 m. Most hydrographic profiles show a sharp thermocline between $10-15 \, m$ depth with temperature increasing to $1.0-2.5 \, °C$. This warmer water below the SO also coincides with the pycnocline and low sediment concentrations, suggesting that water near the glacier between $10-25 \, m$ depth is the displaced, solar-radiated and more saline fjord surface water (SW) mass below the overflow (Svendsen *et al.* 2002; MacLachlan *et al.* 2007). Below 15 m depth salinity increases while sediment concentration decreases, both to relatively constant values. In all profiles below at least 28 m depth, temperature slowly decreases to a constant value of around $0 \, °C$ and salinity increases to a constant of about 34‰. Svendsen *et al.* (2002) defined a similar water mass as the local water (LW) mass, suggesting it is caused by convection as the warmer SW flows along the glacier face, cools and sinks.

A secondary meltwater source from the glacial complex is a submarine meltwater upwelling originating from Kongsvegen. Subglacial meltwater exits Kongsvegen as a turbulent fountain *c.* 0.5 m in height above the delta plain. This water flows across the recently formed ice-contact delta (Figs 3 & 4c)

Table 1. *Sediment yields and erosion rates calculated from grounding-line landforms deposited over the last c.* 20 years

Glaciers	Total glacier basin area (km^2)	Sediment yield (tonnes km^{-2} a^{-1})	Effective erosion rate (mm a^{-1})
Kronebreen, Infantfonna and tributaries	590	1.40×10^3	0.56
Kongsvegen, Sidevegen, Bontfjellbreen and tributaries	210	1.06×10^4	4.24
Total	800	1.20×10^4	4.80

Note: Glacier basin area represents the entire drainage areas for the main glaciers and their tributaries within a single divide. The Kongsvegen basin area incorporates the area of small, sidewall glaciers to the south that have potentially contributed to delta growth.

before entering the fjord, where it forms a buoyant and brackish overflow (SO water mass) (Fig. 5b).

The SO from Kongsvegen is confined to the upper 6 m and is stratified with respect to temperature, salinity and suspended sediment concentration. Salinity is the dominant stratification, with temperature and sediment concentrations displaying greater variance. Sediment concentrations are greatest at the surface, as is the variance in total suspended sediment. The highest measured suspended sediment concentration was 0.081 kg m^{-3} (Table 3); however, calibrated OBS measurements were as high as 0.392 kg m^{-3} (Fig. 5b). Two secondary peaks in sediment concentration were measured with water samples and hydrographic profiles around 12–15 m depth. If these were an interflow it is expected that the higher density sediment layers would be associated with warmer or fresher water than the surrounding water to maintain appropriate density. We therefore infer these higher suspended sediment concentrations within the fjord water column to represent distinct layers of particles settling from the overflow (cf. Cowan & Powell 1991). The warmer and more saline displaced fjord SW is recorded on most profiles below the SO layer and transitions into LW at depths below 28 m.

At 4–5 km from the glaciers, the water column is dominantly stratified with respect to salinity and suspended sediment concentration; however, the thermocline is more poorly defined than in the innermost basin. The influence of solar radiation is obvious with surface temperatures in excess of 5 °C. Surface salinities are as low as 25‰, likely reflecting a combination of glacial and paraglacial meltwater inputs and iceberg melting. Suspended sediment is much lower than in the proximal basin and peaks around 0.02 kg m^{-3}.

Sediment flux to innermost Kongsfjorden

Sedimentation rates vary greatly both with distance from the Kronebreen upwelling and vertically through the water column. Two traps were proximal to the Kronebreen upwelling: ST6a at *c.* 240 m distance and ST3b at *c.* 470 m distance (Fig. 4). The highest vertical accumulation rate, or actual amount of sediment captured per deployment period, was measured in the upper moorings of ST6a and ST3b (Table 4). As is predictable, the lowest accumulation rates occurred in the bottom traps of these moorings. In order to quantify the volume of sediment being deposited on the fjord floor, minimum annual sedimentation rates were calculated using only data from the bottom traps of each mooring. Using the conservative annual melt season of 60 days previously described, linear extrapolation produces a minimum annual (dry) sedimentation rate for sediment traps ST6a and ST3b, respectively, of 4.05×10^5 g m^{-2} a^{-1} (305.29 mm a^{-1}) and 4.88×10^4 g m^{-2} a^{-1} (63.48 mm a^{-1}) (Table 4).

The highest measured sedimentation rates (14.3 mm d^{-1}) occurred in ST6a at a depth of 10 m. At 5 m above the seafloor the daily vertical accumulation rate was about a third of the upper traps at 5.09 mm d^{-1}, still a significant quantity of sediment. The high flux of sediment suggests the grounding-line fan (Fig. 4 GLF) is aggrading at a minimum of 300 mm a^{-1} and likely an even greater rate closer to the grounding line. At this rate, if all variables such as annual sediment flux, upwelling position, relative terminus stability and fan slope stability remain constant, the grounding-line fan will emerge above water in *c.* 18 years.

Two suspended sediment traps recorded sediment flux in proximity to the delta point source in addition to a distal signature of the Kronebreen plume. Sediment trap ST5a was located about 200 m from the low tide level on the delta plain, and ST4a was located equidistance from both the delta and the Kronebreen upwelling at *c.* 1200 m from each (Fig. 4). Sediment accumulation at both moorings was greatest in the bottom traps indicating a pronounced contribution from sediment gravity
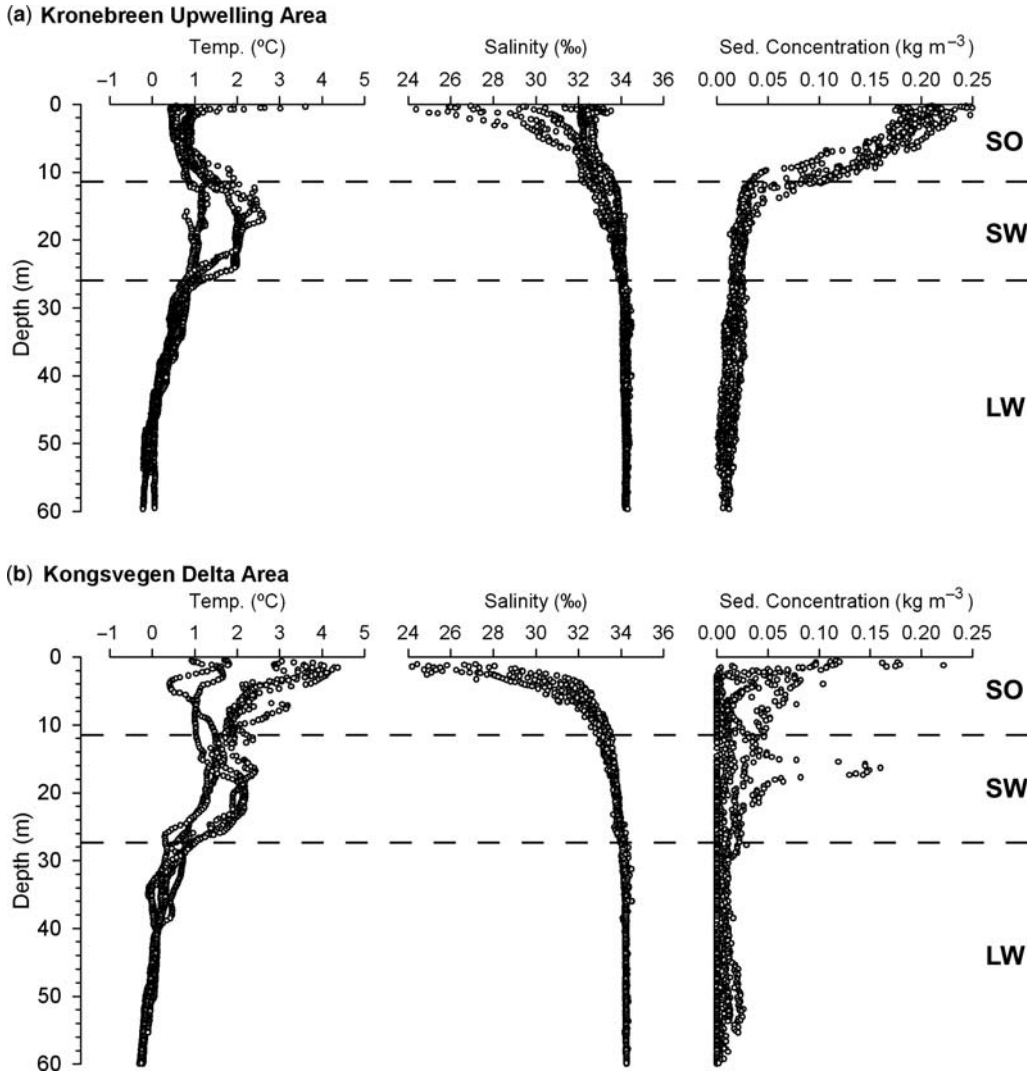
(a) Kronebreen Upwelling Area

(b) Kongsvegen Delta Area

Fig. 5. Composite of CTD profiles for both primary sediment sources with water masses indicated (SO, surface overflow; SW, surface water; LW, local water; nomenclature adapted from Svendsen *et al.* 2002).

flows off the delta front relative to SO contributions (Table 4). ST5a in particular had 72% more sediment in the lower traps compared to the middle traps. Therefore, when calculating a minimum annual sedimentation rates for ST5a, the middle trap data are used. Using the methods outline above, the minimum annual sedimentation rates for sediment traps ST5a and ST4a, respectively, were $7.54 \times 10^4 \, \text{g m}^{-2} \, \text{a}^{-1}$ (69.38 mm a^{-1}) and $9.50 \times 10^4 \, \text{g m}^{-2} \, \text{a}^{-1}$ (88.33 mm a^{-1}) (Table 4).

Suspended sediment traps act not only as a gauge for sedimentation rates, but also indicate where sediment is being transported within the water

column and the carrying capacity of the surface overflow. As expected, suspended particle size decreases rapidly with distance from the source. At mooring ST6a (240 m distance) mean particle size for the upper sediment traps was 172.9 µm (fine-grained sand) and contained sediment as large as medium-grained sand. At ST3b (470 m distance), mean particle size in the upper traps was only 80 µm (very fine-grained sand). Furthermore, all three trap levels at mooring ST6a captured fine-grained sand which composed 56% of the top traps, whereas the upper traps of ST3b contained only 23% fine-grained sand. This trend reveals

Table 2. *Measured water sample suspended sediment concentrations for the Kronebreen glacial upwelling area*

Collection depth (m)	Number of samples	Average concentration (kg m^{-3})	Minimum concentration (kg m^{-3})	Maximum concentration (kg m^{-3})	Standard deviation (kg m^{-3})
0	4	0.102	0.016	0.140	0.058
2	4	0.079	0.031	0.104	0.034
4	1	0.157	0.157	0.157	–
6	1	0.085	0.085	0.085	–
8	1	0.055	0.055	0.055	–
10	1	0.051	0.051	0.051	–
15	2	0.037	0.024	0.049	0.017
20	5	0.030	0.021	0.049	0.011
30	1	0.026	0.026	0.026	–
35	5	0.017	0.007	0.027	0.007
45	1	0.010	0.010	0.010	–
55	3	0.010	0.008	0.012	0.003

that although sediment as large as medium-grained sand is actively transported up to the fjord surface via the subglacial jet and plume, it quickly falls out of suspension.

ST3b had nearly identical mean particle sizes in the middle and upper traps of 80 μm (very fine-grained sand); however, the lower traps captured a mean particle size of 34.8 μm (silt). This trend shows that the smallest particle size fractions, silt and clay, are held mostly in suspension at 470 m distance and are carried farther out into the fjord. The presence of primarily very fine-grained sand but also coarser particles in the top traps, and their significant lack in the lowest traps, shows that these coarser particles are travelling in suspension beyond 470 m which is greater than the 200–300 m estimate of Elverhøi *et al.* (1980).

For ST5a and ST4a, the traps within direct influence of the deltaic runoff, temporal changes in particle transport were also evident. The trap nearest to the delta, ST5a (200 m distance), captured a mean particle size of silt in the upper and middle traps and very fine-grained sand in the lower traps. The coarser sediment in the lower traps is likely a reflection of sediment gravity flows off the delta front. At the more distal ST4a (1200 m distance), the traps all captured at least 5% very fine sand or larger particles. Because of its distance from both sediment point sources, iceberg rafting is believed to contribute the larger particle fractions. However, suspension settling was the dominant process captured at ST4a, with the upper and middle traps recording mean particle sizes of silt and the lower traps capturing mostly clay.

High-resolution particle size analyses conducted on an upper trap in ST6a reveals a cyclic trend in sediment size (Fig. 6). Mean particle size as measured at discrete intervals in the sediment trap fluctuates according to time of day. Deposition time at different points in the trap sediment column

Table 3. *Measured water sample suspended sediment concentrations for the Kongsvegen delta area*

Collection depth (m)	Number of samples	Average concentration (kg m^{-3})	Minimum concentration (kg m^{-3})	Maximum concentration (kg m^{-3})	Standard deviation (kg m^{-3})
2	3	0.054	0.014	0.081	0.035
4	1	0.008	0.008	0.008	–
8	1	0.007	0.007	0.007	–
15	1	0.037	0.037	0.037	–
20	2	0.019	0.006	0.036	0.018
25	1	0.012	0.012	0.012	–
30	1	0.015	0.015	0.015	–
35	3	0.019	0.013	0.031	0.011
40	1	0.016	0.016	0.016	–
55	1	0.010	0.010	0.010	–

Table 4. *Sedimentation rates measured from inner Kongsfjorden, July 2005*

Mooring number trap location	Sampling period (dates) (total hours) (total days)	Average sediment collected (mm)	Average VAR (mm d^{-1})	Average minimum VAR (mm a^{-1})	Average minimum sed. rate (g m^{-2} d^{-1})	Average minimum sed. rate (g m^{-2} a^{-1})
ST6a top	27/7–30/7	43.8	14.29	305.29	6745	4.05×10^5
ST6a mid	73.6 hours	23.6	7.70			
ST6a bot	3.07 days	15.6	5.09			
ST3b top	23/7–27/7	11.3	2.90	63.48	814	4.88×10^4
ST3b mid	93.65 hours	4.88	1.26			
ST3b bot	3.90 days	4.10	1.06			
ST4a top	23/7–28/7	6.25	1.29	88.33	1583	9.50×10^4
ST4a mid	116.23 hours	5.25	1.08			
ST4a bot	4.84 days	7.13	1.47			
ST5a top	24/7–28/7	3.75	0.94	69.38	1257	7.54×10^4
ST5a mid	96.03 hours	4.63	1.16			
ST5a bot	4.00 days	16.17	4.04			

Note: Averages were obtained using four trap measurements at each depth on a particular mooring. Minimum VAR and sedimentation rates were calculated using data from bottom traps, except for ST5A where the middle trap data were used. Sedimentation rates were calculated using dried sediment weights. Annual numbers were determined assuming a melt season of 60 days.
Abbreviation: VAR, vertical accumulation rate.

is inferred by assuming a linear sedimentation rate between the known times of deployment and recovery. Mean particle size in the trap shows a pattern of coarser particles transported and deposited during mid-to-late afternoon hours and smaller particles accumulating during early morning and night hours. On average, the change in mean particle size for these different peaks is 12.3%. Significantly, this cyclic particle size pattern does not appear to be related to fluctuations in one single size fraction, which would negate a linear sedimentation rate

assumption. Rather, the cyclicity represents changes in fractions of sand, silt and clay combined. Furthermore, the fluctuation does not appear related to tidal cycles as has been found in temperate Alaskan fjords with macrotidal fluctuations (Mackiewicz *et al.* 1984; Cowan & Powell 1990).

Although this is an inferred polythermal glacier and the subglacial conduit supplying the suspended sediment is under thick ice, the most logical forcing of the particle size variability based on event timing at this frequency is diurnal temperature
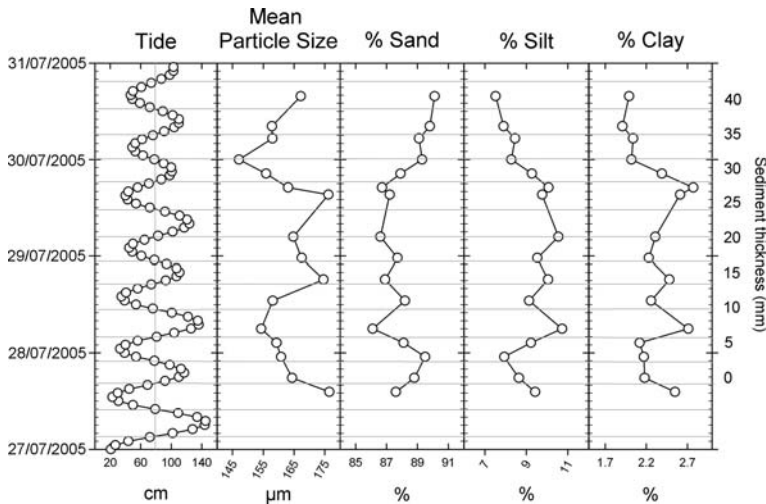

Fig. 6. Cyclic particle size fluctuations as recorded in a top trap from mooring ST6a inferred to represent diurnal discharge variations.

fluctuations. These fluctuations likely drive variations in discharge strength and turbulence with associated changes in travel distance of different particle sizes, resulting in the mean particle size cyclicity associated with time of day.

Discussion

Water column

The Kronebreen meltwater plume and Kongsvegen delta runoff both form buoyant overflows; however, there are several distinctions between the two sources. The SO water mass at the Kronebreen upwelling area has a higher average salinity and more variance than at the delta area. This signature is a result of direct deltaic freshwater flow from Kongsvegen to the surface of the fjord; at the Kronebreen source, however, meltwater turbulently mixes with saline fjord water as it rises to the surface (cf. Syvitski 1989; Powell 1990). The Kronebreen efflux has previously been postulated to mix in crevasses extending back from the grounding line prior to exiting the glacier (Elverhøi et al. 1980); however, the current stream when studied was discharging from a shear face at the grounding line. Another distinction between the deltaic and upwelling sources is that water characterized above 12 m water depth in the upwelling area shows more uniform temporal temperature patterns and is 2 °C colder than water from the delta. Also significantly, the Kronebreen upwelling area generally had higher average sediment concentrations and less variance in that parameter over time in the upper 12 m of water compared to those recorded in the delta area. These characteristics show the upwelling from Kronebreen had a more uniform higher velocity and locally concentrated discharge of sediment and meltwater throughout the sampling period relative to the deltaic runoff.

The deltaic overflow plume, with higher variability in temperature and sediment concentration, shows more susceptibility to surface processes as it flows over the delta and into the fjord. Another major distinction in the SO profiles is thickness of the overflow; from the upwelling it is c. 12 m thick, whereas the overflow at the delta is c. 7 m thick. This difference in thickness indicates a larger volume of water flowing out from the Kronebreen subglacial meltwater upwelling compared to the relatively smaller volume flowing from the marginal Kongsvegen fountain and over the delta.

Spatial and temporal variability also exists in the deeper (12–28 m depth) SW mass. At both sites, two distinct temperature trends exist in the SW water mass: one of lower temperatures c. 1.2 °C and a second at c. 2.4 °C (see Fig. 5a, b). We speculate this difference reflects surface conditions: solar radiation, meteorological conditions, dominant wind direction and dominant current direction that alter the spatial extent of SW before it is displaced by the SO. Sediment concentration profiles through the SW mass in the Kronebreen area again show a very uniform spatiotemporal distribution, whereas those in the Kongsvegen delta area show variations that reflect predominant surface conditions.

The deepest water mass, LW (28 m depth to the fjord floor), shows uniformity at both locations (Fig. 5a, b). The profiles reflect a stable interval of the water column not affected by surface conditions. It is through this interval that suspended sediments settle calmly to the fjord floor.

Suspended sediment concentrations from calibrated OBS data in July 2005 peaked at 0.39 kg m^{-3}; however, most overflow samples were around 0.20–0.25 kg m^{-3} which are lower than found in other studies (e.g. 0.34 kg m^{-3} in Svendsen et al. 2002 and 0.50 kg m^{-3} in Elverhøi et al. 1980). However, our measured concentrations were higher than another recent study (maximum 0.1 kg m^{-3} near Kronebreen in Aliani et al. 2004). Our actual sediment concentrations were probably much higher, however, as shown by our sediment trap records. The relatively low concentrations in our measured water samples used to calibrate the OBS data may skew our data to the lower end of the suspended sediment spectrum. This would result if our samples were not collected in the highest concentrations of suspended sediments in the plume. Alternatively, although speculative, the lower suspended sediment concentrations but higher sediment fluxes may indicate higher total meltwater with an average sediment load relative to the other studies. This hydrologic scenario would result in dilution and less sediment per unit volume of water, but higher sedimentation rates because of increased discharge.

Sediment flux spatial variation

The interplay and dynamics of the two meltwater sources is indicated by varied suspended sediment loads recorded in sediment traps and hydrographic profiles. Traps proximal to the Kronebreen upwelling plume (ST6a, ST3b) captured most sediment in their upper traps, whereas traps positioned near the deltaic runoff (ST4a, ST5a) predominantly captured sediment in the lowest traps. High suspended sediment load in the Kronebreen overflow resulted in the disproportionate sediment captured in upper traps. Although the Kronebreen SO water is more turbulently mixed relative to the deltaic SO, the plume and overflow velocities are sufficient to maintain high sediment concentrations thus resulting in a smaller relative volume of sediment immediately released from suspension. Rather, this

material is transported more distally beyond the lower traps in the immediate upwelling area to a point where overflow velocity sufficiently decreases and causes particle release to the lower water column.

In contrast, traps positioned to primarily capture deltaic runoff (ST4a, ST5a) received a smaller volume of suspended sediment from the SO in their upper traps. Also in these traps, sediment gravity flows appear more frequent, contributing significantly to the relatively larger volume of sediment captured in bottom traps. For example, ST5a anchored to the delta front with bottom traps at 5 m above the floor contained numerous sand laminae from sediment gravity flows. ST4a, in contrast, located farther from the delta and on relatively flat seafloor, contained only silt and clay in its lower traps. Here, we interpret increased sediment volume in the lower traps to predominantly reflect suspension settling. At this location we also infer a small sediment component contributed by distal, low-viscosity gravity flows that compositionally indicate they are sourced from the Kronebreen grounding-line fan. Such slides, slumps and sediment gravity flows are common at Alaskan tidewater termini because of slope over-steepening by high sedimentation rates and disruption of bottom sediment from glacier pushing and iceberg calving (Powell 1981). However, higher overall sedimentation rates at ST4a indicate it is influenced by both sources (Table 4).

Local and global sediment flux perspectives

Daily sediment flux recorded as dry weights and accumulation thicknesses in this study are higher than those from previous studies at nearby glaciers. Our highest sediment flux of 1.86×10^4 g m^{-2} d^{-1} (14.3 mm d^{-1}) was measured at a depth of 10 m at a distance 240 m from Kronebreen. This value is two orders of magnitude higher than the highest fluxes of other studies in inner Kongsfjorden (800 g m^{-2} d^{-1} measured at 15 m depth, 250 m from Kongsbreen in Svendsen *et al.* 2002 and 933 g m^{-2} d^{-1} measured at 15 m depth, 300 m from Kongsbreen in Zajaczkowski 2002). Our minimum fluxes were both from bottom traps: 6.74×10^3 g m^{-2} d^{-1} at 240 m and 813 g m^{-2} d^{-1} at 470 m distance from Kronebreen. The latter was the lowest measured sediment flux, a value comparable to the maximum near-surface values recorded in other studies.

When we extrapolate our measured sedimentation rates to a conservative 60-day melt season, our results are similar to those of some previous studies but are higher than others. Elverhøi *et al.* (1980) measured rates in cores to be 100 mm a^{-1} wet mud or 30 mm a^{-1} dry sediment, and 50–100 mm a^{-1} within 10 km from the glacier (Elverhøi *et al.* 1983). These are similar values to those we estimate, where minimum sediment accumulation rates are 60–90 mm a^{-1} at <0.5 km from point source depocentres. Our annual sedimentation rates at the glacier front are a minimum of 4.05×10^5 g m^{-2} a^{-1} with an inner basin average of 1.56×10^5 g m^{-2} a^{-1}. These annual rates are an order of magnitude higher than those of other studies in inner Kongsfjorden: 1.80×10^4 g m^{-2} a^{-1} measured near Ossian Sarsfjellet using ^{210}Pb$_{ex}$ dating of sediment cores (Aliani *et al.* 2004), 2.0×10^4 g m^{-2} a^{-1} measured for the Kongsbreen 'glacier front' using ^{210}Pb$_{ex}$ dating of sediment cores (Svendsen *et al.* 2002) and 5.6×10^4 g m^{-2} a^{-1} measured in sediment traps at 15 m depth, 300 m from Kongsbreen (from daily rates in Zajaczkowski 2002 multiplied by a 60-day melt season). Higher rates of this study may indicate a higher relative meltwater and sediment flux of the Kronebreen–Kongsvegen glacier complex compared to the other nearby glaciers measured in other studies. These results are expected given that Kongsbreen drains only about 42% of the total area of Kronebreen. Sediment flux has been shown to generally scale with glacier basin size in Alaska (Powell 1991) and worldwide (Hallet *et al.* 1996), although others argue the basin area–erosion relationship is too simple (Elverhøi *et al.* 1998). It is also possible that measurements in other studies were taken at greater distance and are therefore expected to be significantly lower (e.g. Cai 1994; Cowan *et al.* 1999).

Our measured sediment fluxes from Kronebreen and Kongsvegen fall within the range of those for other subpolar polythermal glaciers when placed within the spectrum of glacial regimes. For example, the maximum sediment flux from temperate glaciers in southeastern Alaska is at least one order of magnitude higher than for Kronebreen. For McBride Glacier in Alaska, Cowan & Powell (1991) measured maximum and average sediment fluxes of 2.4×10^5 g m^{-2} d^{-1} and 5.3×10^4 g m^{-2} d^{-1}, respectively, into ice-proximal McBride Inlet. Both are at least one order of magnitude higher than the ice-proximal rates for Kongsfjorden (Table 4). At the opposite end of the spectrum are polar regime glaciers. A recent sediment flux measured on the Antarctic Peninsula was recorded at $1.7–3.5 \times 10^3$ g m^{-2} a^{-1} (Gilbert *et al.* 2003), one order of magnitude less than the subpolar glaciers of this study (Table 4).

Sediment yields calculated from volumes of ice-contact depositional landforms are 1.40×10^3 tonnes km^{-2} a^{-1} for Kronebreen and 1.06×10^4 tonnes km^{-2} a^{-1} for Kongsvegen (1.20×10^4 tonnes km^{-2} a^{-1}, or 4.80 mm a^{-1} of effective bedrock erosion combined) (Table 1). The majority of this contribution comes from very rapid building of the Kongsvegen ice-contact delta. This yield is about a factor of five greater than the 30-year

average estimated by Elverhøi *et al.* (1998), but is still at least an order of magnitude less than temperate Alaskan glaciers (Hallet *et al.* 1996; Elverhøi *et al.* 1998). The Kongsvegen yield represents an ice-contact measurement and, since sediment accumulation rates decrease according to power and exponential decay functions with distance (Cai 1994; Cowan *et al.* 1999), these data are considered compatible with other measurements obtained farther from the glacier termini. Indeed, our own sediment trap data collected farther from the termini produce sediment accumulation rates similar to the longer term averages of nearby studies. Due to their close glacier proximity, these yields are therefore very rare and represent the true erosive ability of these subpolar glaciers.

Conclusions

Retreat of the Kronebreen–Kongsvegen glacier complex has significantly slowed in recent decades due to post-surge quiescent-phase conditions. Hydrographic profiles record the mixing of fjord and glacial waters including the transport and rainout of suspended sediments, closer than previously documented. Sediment trap data show that Kronebreen is now the major suspended sediment source as opposed to Kongsvegen, a relationship that has reversed within the last 25 years. Glacifluvial deltaic runoff from Kongsvegen presently contributes only 20–25% of the total volume of sediment in the inner fjord basin. The submarine discharge from Kronebreen contributes the remainder. Measured daily sediment fluxes are higher than those presented by previous researchers. However, when extrapolated for a full melt season, minimum annual vertical accumulation rates are similar to some previous estimates but higher than others. We expect this difference reflects the larger relative glacierized drainage area of the Kronebreen–Kongsvegen complex compared to other nearby glaciers. Most of the inner fjord basin away from point sources receives at least 60–90 mm a^{-1} of sediment from suspension settling.

Bathymetric profiling reveals a grounding-line fan adjacent to the major submarine meltwater discharge of Kronebreen. Near-bottom sediment traps indicate it is actively building at more than 300 mm a^{-1}. If terminus and subglacial conduit stability ensues, at this rate of aggradation the fan will emerge from the fjord in *c.* 18 years. An ice-contact delta in the southeastern fjord corner has built at a rate of 8.91×10^5 m^3 a^{-1}, providing an important and rare estimate of fully ice-contact glacial debris flux. Combined, these landforms equate to 4.80 mm a^{-1} of effective bedrock erosion for the glacial complex. This is almost an ice-contact value and therefore represents the full capacity of

these subpolar polythermal glaciers in landscape denudation.

With continued climatic warming we expect the ablation season of Kronebreen and Kongsvegen to grow. Meltwater and therefore sediment flux may also increase. Under warming conditions we would expect greater sedimentation rates and faster infilling of the inner basin of Kongsfjorden. If the terminus remains relatively stable, it is expected that an ice-contact delta will form in front of Kronebreen as it has for Kongsvegen. We expect these landforms will enhance glacier margin stability and the ability of the terminus to re-advance in future if ice mass-balance permits. This may occur during initial stages of climate warming if precipitation increases, causing mass-balance to become less negative.

References

ALIANI, S., BARTHOLINI, G. ET AL. 2004. Multidisciplinary investigations in the marine environment of the inner Kongsfiord, Svalbard islands (September 2000 and 2001). *Chemistry and Ecology*, **20**, S19–S28.

ALLEY, R. B. 1991. Sedimentary processes may cause fluctuations of tidewater glaciers. *Annals of Glaciology*, **15**, 119–124.

ALLEY, R. B., ANANDAKRISHNAN, S., DUPONT, T. K., PARIZEK, B. R. & POLLARD, D. 2007. Effect of sedimentation on ice-sheet grounding-line stability. *Science*, **315**, 1838–1841.

CAI, J. 1994. *Sediment yields, lithofacies architecture, and mudrock characteristics in glacimarine environments*. PhD thesis, Northern Illinois University, DeKalb, Illinois, USA.

COTTIER, F., TVERBERG, V., INALL, M., SVENDSEN, H., NILSEN, F. & GRIFFITHS, C. 2005. Water mass modification in an Arctic fjord through cross-shelf exchange: the seasonal hydrography of Kongsfjorden, Svalbard. *Journal of Geophysical Research*, **110**, C122005, doi: 10.1029/2004JC002757.

COWAN, E. A. 1988. *Sediment transport and deposition in a temperate glacial fjord, Glacier Bay, Alaska*. PhD Thesis, Northern Illinois University, Illinois, USA.

COWAN, E. A. & POWELL, R. D. 1990. Suspended sediment transport and deposition of cyclically interlaminated sediment in a temperate glacial fjord, Alaska, U.S.A. *In*: DOWDESWELL, J. A. & SCOURSE, J. D. (eds) *Glacimarine Environments: Processes and Sediments*. Geological Society, London, Special Publications, **53**, 75–89.

COWAN, E. A. & POWELL, R. D. 1991. Ice-proximal sediment accumulation rates in a temperate glacial fjord, southeastern Alaska. *In*: Anonymous (ed.) *Glacial Marine Sedimentation: Paleoclimatic Significance*.

Geological Society of America, Special Paper, **261**, 61–73.

COWAN, E. A., SERAMUR, K. C., CAI, J. & POWELL, R. D. 1999. Cyclic sedimentation produced by fluctuations in meltwater discharge, tides and marine productivity in an Alaskan fjord. *Sedimentology*, **46**, 1109–1126.

ELVERHØI, A., LIESTØL, O. & NAGY, J. 1980. Glacial erosion, sedimentation and microfauna in the inner part of Kongsfjorden, Spitsbergen. *Norsk Polarinstitutt Skrifter*, **172**, 28–61.

ELVERHØI, A., LØNNE, O. & SELAND, R. 1983. Glacio-marine sedimentation in a modern fjord environment, Spitsbergen. *Polar Research*, **1**, 127–149.

ELVERHØI, A., HOOKE, R. LeB. & SOLHEIM, A. 1998. Late Cenozoic erosion and sediment yield from the Svalbard-Barents Sea region: implications for understanding erosion of glacierized basins. *Quaternary Science Reviews*, **17**, 209–241.

FISCHER, M. P. & POWELL, R. D. 1998. A simple model for the influence of push-morainal banks on the calving and stability of glacial tidewater termini. *Journal of Glaciology*, **44**, 31–41.

GERLAND, S., HAAS, C., NICOLAUS, M. & WINTHER, J.-G. 2004. Seasonal development of structure and optical surface properties of fast ice in Kongsfjorden, Svalbard. *Reports on Polar and Marine Research*, **129**, 26–34.

GILBERT, R., CHONG, A., DUNBAR, R. B. & DOMACK, E. W. 2003. Sediment trap records of glacimarine sedimentation at Müller Ice Shelf, Lallemand Fjord, Antarctic Peninsula. *Arctic, Antarctic, and Alpine Research*, **35**, 24–33.

HAGEN, J. O., LIESTØL, O., ROLAND, E. & JØRGENSEN, T. 1993. Glacier atlas of Svalbard and Jan Mayen. *Norsk Polarinstitutt Meddeleser*, **129**, 141.

HAGEN, J. O., MELVOLD, K., PINGLOT, F. & DOWDESWELL, J. A. 2003. On the net mass balance of the glaciers and ice caps in Svalbard, Norwegian Arctic. *Arctic, Antarctic, and Alpine Research*, **35**, 264–270.

HALD, M., EBBESEN, H. ET AL. 2004. Holocene paleoceanography and glacial history of the West Spitsbergen area, Euro-Arctic margin. *Quaternary Science Reviews*, **23**, 2075–2088.

HALLET, B., HUNTER, L. & BOGEN, J. 1996. Rates of erosion and sediment evacuation by glaciers: a review of field data and their implications. *Global and Planetary Change*, **12**, 213–235.

HJELLE, A. 1993. *Geology of Svalbard*, Norsk Polarinstitutt Oslo.

HODSON, A., GURNELL, A., TRANTER, M., BOGEN, J., HAGEN, J. O. & CLARK, M. 1998. Suspended sediment yield and transfer processes in a small high-Arctic glacier basin, Svalbard. *Hydrological Processes*, **12**, 73–86.

HOP, H., PEARSON, T. ET AL. 2002. The marine ecosystem for Kongsfjorden, Svalbard. *Polar Research*, **21**, 167–208.

HOWE, J. A., MORETON, S. G., MORRI, C. & MORRIS, P. 2003. Multibeam bathymetry and depositional environments of Kongsfjorden and Krossfjorden, western Spitsbergen, Svalbard. *Polar Research*, **22**, 301–316.

INGÓLFSSON, O. 2004. Outline of the geography and geology of Svalbard. *UNIS Course Packet*. UNIS.

IPCC 2007. Summary for Policymakers. *In*: SOLOMON, S., QIN, D., MANNING, M., CHEN, Z., MARQUIS, M., AVERYT, K. B., TIGNOR, M. & MILLER, H. L. (eds) *Climate Change 2007: The Physical Science Basis. Contribution of Working Group I to the Fourth Assessment Report of the Intergovernmental Panel on Climate Change*. Cambridge University Press, Cambridge.

LAMB, H. H. 1977. *Climate: Present, Past and Future*, Methuen, London.

LEFAUCONNIER, B., HAGEN, J. O. & RUDANT, J. P. 1994. Flow speed and calving rate of Kongsbreen glacier, Svalbard, using SPOT images. *Polar Research*, **13**, 59–65.

MACKIEWICZ, N. E., POWELL, R. D., CARLSON, P. R. & MOLNIA, B. F. 1984. Interlaminated ice-proximal glacimarine sediments in Muir Inlet, Alaska. *Marine Geology*, **57**, 113–147.

MACLACHLAN, S. E., COTTIER, F. R., AUSTIN, W. E. N. & HOWE, J. A. 2007. The salinity: del^{18}O water relationship in Kongsfjorde, western Spitsbergen. *Polar Research*, **26**, 160–167.

MEIER, M. F. & POST, A. 1969. What are glacier surges? *Canadian Journal of Earth Science*, **6**, 807–817.

MELVOLD, K. & HAGEN, J. O. 1998. Evolution of a surge-type glacier in its quiescent phase; Kongsvegen, Spitsbergen, 1964–95. *Journal of Glaciology*, **44**, 394–404.

POWELL, R. D. 1981. A model for sedimentation by tidewater glaciers. *Annals of Glaciology*, **2**, 129–134.

POWELL, R. D. 1984. Glacimarine processes and inductive lithofacies modelling of ice shelf and tidewater glacier sediments based on Quaternary examples. *Marine Geology*, **57**, 1–52.

POWELL, R. D. 1990. Glacimarine processes at grounding-line fans and their growth to ice-contact deltas. *In*: DOWDESWELL, J. A. & SCOURSE, J. D. (eds) *Glacimarine Environments: Processes and Sediments*. Geological Society, London, Special Publications, **53**, 53–73.

POWELL, R. D. 1991. Grounding-line systems as second-order controls on fluctuations of tidewater termini of temperate glaciers. *Glacial Marine Sedimentation; Paleoclimatic Significance*. Geological Society of America, Special Paper, **261**, 75–94.

POWELL, R. D. & ALLEY, R. B. 1997. Grounding-line systems; processes, glaciological inferences and the stratigraphic record. *In*: BARKER, P. F. & COOPER, A. C. (eds) *Geology and Seismic Stratigraphy of the Antarctic Margin, 2, Antarctic Research Series*. AGU, Washington, DC, **71**, 169–187.

SUND, M. 2007. Calving front of Kronebreen, Svalbard in July 2007. http://www.geo.uio.no/glaciodyn/Publications/Kronebreen.wmv.

SVENDSEN, H., BESZCZYNSKA-MØLLER, A. ET AL. 2002. The physical environment of Kongsfjorden-Krossfjorden, an Arctic fjord system in Svalbard. *Polar Research*, **21**, 133–166.

SYVITSKI, J. P. M. 1989. On the deposition of sediment within glacier-influenced fjords: oceanographic controls. *Marine Geology*, **85**, 301–329.

WOODWARD, J., MURRAY, T., CLARK, R. A. & STUART, G. W. 2003. Glacier surge mechanisms inferred from ground-penetrating radar; Kongsvegen, Svalbard. *Journal of Glaciology*, **49**, 473–480.

ZAJACZKOWSKI, M. 2002. On the use of sediment traps in sedimentation measurements in glaciated fjords. *Polish Polar Research*, **23**, 161–174.